Biochemical and Biophysical Research Communications 463 (2015) 818–824

Contents lists available at ScienceDirect

Biochemical and Biophysical Research Communications

journal homepage: www.elsevier.com/locate/ybbrc

In vivo cardiac glucose metabolism in the high-fat fed mouse: Comparison of euglycemic–hyperinsulinemic clamp derived measures of glucose uptake with a dynamic metabolomic flux profiling approach

Greg M. Kowalski [a, *], David P. De Souza [b], Steve Risis [c], Micah L. Burch [d], Steven Hamley [a], Joachim Kloehn [b], Ahrathy Selathurai [a], Robert S. Lee-Young [c], Dedreia Tull [b], Sean O'Callaghan [b], Malcolm J. McConville [b], Clinton R. Bruce [a]

[a] Centre for Physical Activity and Nutrition Research, School of Exercise and Nutrition Sciences, Deakin University, Burwood, Victoria 3125, Australia
[b] Metabolomics Australia, Department of Biochemistry and Molecular Biology, Bio21 Institute of Molecular Science and Biotechnology, University of Melbourne, Parkville, Victoria 3010, Australia
[c] Cellular and Molecular Metabolism Laboratory, Baker IDI Heart and Diabetes Institute, Melbourne, Victoria 3004, Australia
[d] Brigham and Women's Hospital, Department of Medicine, Boston, MA, USA

ARTICLE INFO

Article history:
Received 27 May 2015
Accepted 2 June 2015
Available online 15 June 2015

Keywords:
Cardiac insulin resistance
Metabolomics
Stable isotopes
Gas-chromatography mass spectrometry

ABSTRACT

Rationale: Cardiac metabolism is thought to be altered in insulin resistance and type 2 diabetes (T2D). Our understanding of the regulation of cardiac substrate metabolism and insulin sensitivity has largely been derived from *ex vivo* preparations which are not subject to the same metabolic regulation as in the intact heart *in vivo*. Studies are therefore required to examine *in vivo* cardiac glucose metabolism under physiologically relevant conditions.
Objective: To determine the temporal pattern of the development of cardiac insulin resistance and to compare with dynamic approaches to interrogate cardiac glucose and intermediary metabolism *in vivo*.
Methods and results: Studies were conducted to determine the evolution of cardiac insulin resistance in C57Bl/6 mice fed a high-fat diet (HFD) for between 1 and 16 weeks. Dynamic *in vivo* cardiac glucose metabolism was determined following oral administration of [U-^{13}C] glucose. Hearts were collected after 15 and 60 min and flux profiling was determined by measuring ^{13}C mass isotopomers in glycolytic and tricarboxylic acid (TCA) cycle intermediates. Cardiac insulin resistance, determined by euglycemic–hyperinsulinemic clamp, was evident after 3 weeks of HFD. Despite the presence of insulin resistance, *in vivo* cardiac glucose metabolism following oral glucose administration was not compromised in HFD mice. This contrasts our recent findings in skeletal muscle, where TCA cycle activity was reduced in mice fed a HFD. Similar to our report in muscle, glucose derived pyruvate entry into the TCA cycle in the heart was almost exclusively via pyruvate dehydrogenase, with pyruvate carboxylase mediated anaplerosis being negligible after oral glucose administration.
Conclusions: Under experimental conditions which closely mimic the postprandial state, the insulin resistant mouse heart retains the ability to stimulate glucose metabolism.

1. Introduction

Cardiac insulin resistance, as demonstrated by a reduction in insulin stimulated glucose uptake into the myocardium, is often present in patients with whole-body insulin resistance and type 2 diabetes (T2D) [1–5]. However, developing an understanding of the mechanisms responsible for cardiac insulin resistance has been challenging due to the obvious limitations in obtaining fresh

Abbreviations: [U-^{13}C] glucose, uniformly carbon-13 labelled glucose; [U-^{13}C] pyruvate, uniformly carbon-13 labelled pyruvate; 3PGA, 3-phosphoglycerate.

* Corresponding author. Centre for Physical Activity and Nutrition Research, School of Exercise and Nutrition Sciences, Deakin University, 221 Burwood Highway, Burwood, Victoria 3125, Australia.
E-mail address: greg.kowalski@deakin.edu.au (G.M. Kowalski).

http://dx.doi.org/10.1016/j.bbrc.2015.06.019
0006-291X/

heart tissue from humans. Thus, is not surprising that together with the emergence of genetic engineering techniques to manipulate the mouse genome, the field of cardio-metabolic research has become increasingly reliant on mouse models. One of the most commonly used models in this field is the chronically high-fat diet (HFD) fed C57Bl/6 mouse, which shows important metabolic changes that resemble the human 'pre-diabetic' condition, including obesity, hyperinsulinemia, insulin resistance and glucose intolerance [6]. We have previously performed detailed time course studies in C57Bl/6 mice investigating the evolution of HFD-induced whole-body and tissue specific (liver, skeletal muscle and adipose) insulin resistance via the use of the 'gold standard' euglycemic–hyperinsulinemic clamp [6]. We found that HFD-induced whole body insulin resistance developed rapidly, within 1 week of HFD feeding, with this being entirely mediated by impaired hepatic insulin action [6]. Extending the HFD to 3 weeks exacerbated the insulin resistance due to the induction of skeletal muscle insulin resistance, however beyond this point, even after 16 weeks of HFD, did not further deteriorate whole-body or organ specific insulin resistance [6]. However, our previous report did not document the temporal development of cardiac insulin resistance [6]. While the clamp remains the 'gold-standard' approach to assess insulin sensitivity, it fails to adequately simulate the dynamic changes in hormones and substrates which occur in the postprandial state. We have recently developed an innovative method to asses intracellular glucose metabolism under the physiologically and clinically relevant condition of the oral glucose tolerance test (OGTT) using dynamic metabolomics [7]. Therefore we aimed to determine the evolution of HFD induced cardiac insulin resistance in the C57Bl/6 mouse using the euglycemic–hyperinsulinemic clamp and to examine how the presence of cardiac insulin resistance impacts on intermediary metabolism under the dynamic physiological conditions of an oral glucose challenge.

2. Methods

2.1. Animals

All experiments were approved by the Monash University Animal Research Platform Animal Ethics Committee or the AMREP Animal Ethics Committee and were in accordance with the National Health and Medical Research Council of Australia Guidelines on Animal Experimentation. Mice were maintained at 22 ± 1 °C on a 12 h light/dark cycle, with free access to food and water. Eight week old male C57BL/6 mice were maintained on a standard chow control diet (9% energy as fat, Barastoc Rat and Mouse, Ridley AgriProducts, Melbourne, Australia) or HFD (42% energy from fat, 20% by weight from sucrose, Specialty Feeds SF4-001, Glen Forrest, WA, Australia) for the duration specified for each study described below.

2.2. Euglycemic-hyperinsulinemic clamp studies

Mice were maintained on the chow or HFD for 1, 3, 6 or 16 weeks. We have previously documented the temporal development of HFD-induced whole-body, liver, skeletal muscle and adipose specific insulin resistance in our previous publication [6]. The data reported here on cardiac glucose uptake during the clamp are derived from studies conducted on these same animals, findings that were not reported on in the original publication [6]. All methods and clamp parameters including glucose turnover rates, plasma glucose and insulin concentrations can be obtained from our previous publication [6]. Briefly, a jugular vein catheter was inserted into mice 4 days before clamp studies. The clamp was performed on 5 h fasted, conscious, restrained mice. Human insulin (ActRapid; Novo Nordisk, Baulkham Hills, New South Wales, Australia) was infused at the rate of 4 mU/kg min. At 120 min, a bolus of [2-^{14}C]-deoxyglucose ([^{14}C]-2DG; 13 μCi; PerkinElmer, Waltham, MA) was administered via the catheter. Blood (10 μL) was taken at 2, 15, 25, and 35 min for the determination of [^{14}C]-2DG. Mice were then anesthetized and heart tissue collected immediately and freeze clamped in liquid nitrogen. The [^{14}C]-2DG radioactivity was determined by liquid scintillation counting. Accumulation of [^{14}C]-2DG was determined in an aqueous extract of tissue after homogenization. The area under the tracer disappearance curve of [^{14}C]-2DG, together with the radioactivity for the phosphorylated [^{14}C]-2DG from the heart tissue was used to calculate the glucose metabolic index (Rg′) [8].

2.3. Oral [U-^{13}C] glucose challenge

All specific details regarding the dynamic metabolomics experiments and analysis can be found in our recent publication which was focused on skeletal muscle [7]. In the studies detailed here, cardiac tissue was obtained from animals in this previous publication [7]. Briefly, mice were fed a chow or HFD for 10 weeks to induce obesity, whole-body and cardiac specific insulin resistance. The 10 week feeding period was selected as it represents an intermediate time point at which cardiac insulin resistance and obesity were both evident (Fig. 1). After a 5 h fast, mice underwent an oral glucose challenge where [U-^{13}C] glucose (50 mg; 25% w/v; 99% enrichment, Sigma Aldrich) was administered to mice via oral gavage. Hearts were collected 15 and 60 min following glucose administration and were immediately frozen in liquid nitrogen. Blood glucose, plasma insulin and other metabolic parameters during the glucose challenges have been previously reported [7].

2.4. Tissue metabolite extraction

All specific details of the extraction can be found in our previous publication [7]. Briefly, heart tissue (10–20 mg) was extracted in 3:1 methanol:water containing 2 nmol scyllo-inositol (internal control) using a Precellys bead-mill with a Cryolys attachment (Bertin Technologies, France). After the addition of chloroform and drying the aqueous (polar) phase, samples were derivatized with 20 μL methoxyamine HCl (30 mg/ml in pyridine) and 20 μL of BSTFA + 1% TMCS (Thermo Fisher Scientific, Waltham, USA).

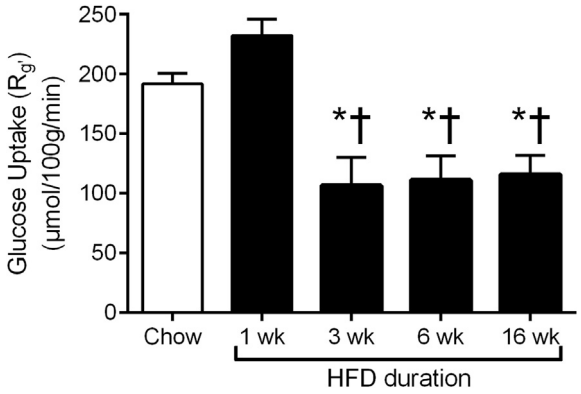

Fig. 1. Effects of HFD feeding on cardiac insulin stimulated glucose uptake. Cardiac glucose uptake (R_g') during the clamp. For ease of presentation, chow data contains all the time points studied as cardiac glucose uptake did not change over time; chow N = 29, HFD N = 5–7/group. *P < 0.05 vs. chow, †P < 0.05 vs 1wk HFD; as determined by one-way ANOVA.

2.5. ^{13}C targeted metabolomics

Targeted metabolomics was performed on the tissue samples using gas chromatography mass spectrometry (GC–MS) as previously detailed [7]. An Agilent HP 7890 GC system equipped with a VF-5ms capillary column with 10 m inert eziguard (J&W Scientific, 30 m, 250 μm inner diameter, 0.25 μm film thickness) and an Agilent 5975 MSD (Agilent Technologies, Santa Clara, USA) in electron ionization (EI) mode was used. ^{13}C glucose derived carbon labelling was determined in key metabolites of the glycolytic and TCA cycle via mass isotopomer peak shift analysis. Specific details of the elution time for each intermediate as well as the fragmentation pattern can be provided on request and can also be found on the NIST database.

2.6. Metabolomic data analysis

Having extracted enriched and unenriched metabolite abundances using Agilent Mass Hunter Quantitative analysis software, Mass Isotopomer Distribution Vectors (MIDVs) were calculated for each fragment [9]. This removes naturally occurring background isotopic labelling from the fragments. The fractional labelling or atomic percent enrichment (APE) in each case was determined by the following equation:

$$APE = \frac{\sum_{i=0}^{n} i \cdot m_i}{n \cdot \sum_{i=0}^{n} m_i}$$

where n represents the number of carbon atoms in the considered fragment and i the mass isotopomers (abundance of M + 0, M + 1, M + 2 … etc.). Thus, the *APE* not only takes into account what proportion of the specific metabolite pool is labelled with ^{13}C, but also the number of ^{13}C atoms incorporated into that specific molecule [10]. The mass isotopomer distribution (MID) is presented as fractional abundance and shows the fraction of the entire specific metabolite pool that is labelled with the exact number of ^{13}C atoms, e.g. M + 2 of 0.2 for fumarate means that 20% of all the fumarate molecules are labelled with two ^{13}C atoms, while M + 0 of 0.7 means that 70% of the fumarate pool contains no ^{13}C atoms (unlabelled). The sum of all MIDs always is equal to one, hence the term fractional abundance. All the above calculations and corrections were calculated by software designed in-house at Metabolomics Australia based on the theory of Nanchen et al. [9].

2.7. Statistical analysis

All data are presented as mean ± standard error of the mean (SEM). Data were analysed by unpaired Student's *t*-test, one-way or two-way factorial ANOVA where appropriate. For the ANOVA procedures, Newman–Keuls post-hoc tests were used to establish differences between groups. Statistical significance was set at $P < 0.05$.

3. Results and discussion

3.1. Temporal pattern of HFD-induced cardiac insulin resistance

We have previously conducted a detailed study documenting the development of whole-body and tissue-specific insulin resistance in mice fed a HFD [6]. In this study male C57BL/6 mice were fed a control chow or HFD for either 1, 3, 6 or 16 weeks after which the euglycemic–hyperinsulinemic clamps were performed at each corresponding time point [6]. In this study, however, we did not report on the effects on cardiac insulin sensitivity. Thus here we have analysed the cardiac tissue from our previous study [6], in order to describe the evolution of HFD induced cardiac insulin resistance. Similar to our observations in skeletal muscle [6], here we report that cardiac glucose uptake was not altered in mice fed a HFD for 1 week (Fig. 1), with defects in glucose uptake only becoming apparent after 3 weeks of the HFD (Fig. 1). Extending the HFD duration to 6 or 16 weeks caused no further decrement in insulin-stimulated cardiac glucose uptake (Fig. 1), which is similar to the findings of Park et al. [11]. Furthermore, these results are

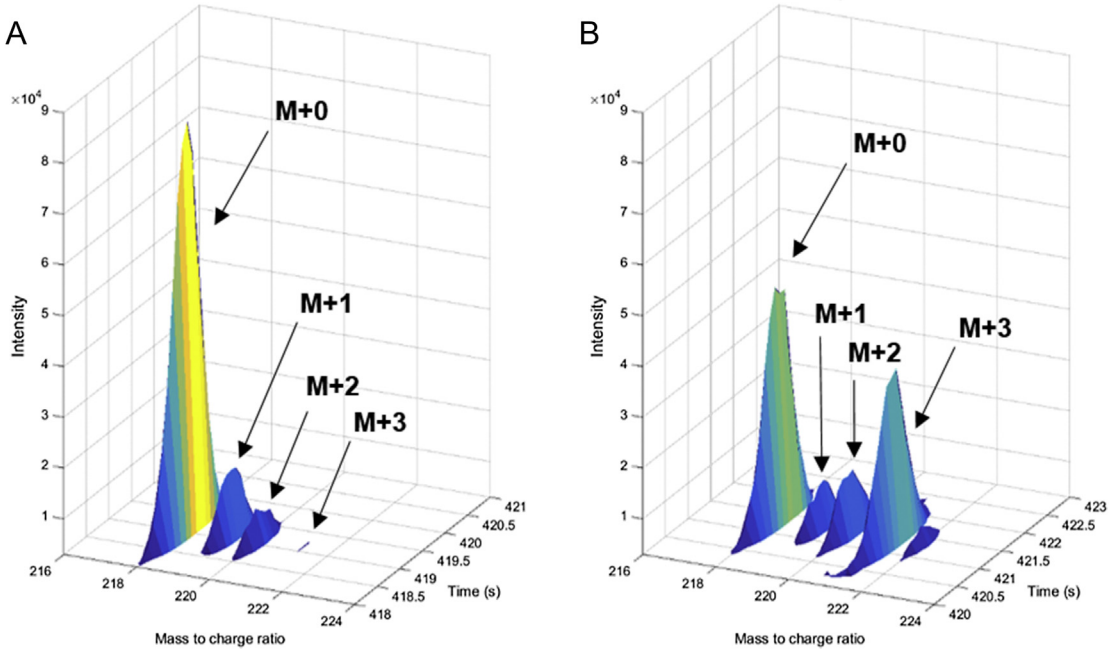

Fig. 2. Visual representation of metabolite labelling. (A) Representative chromatogram of cardiac alanine (218 *m/z* C1–C3 ion) from a mouse 15 min after oral water administration. This demonstrates the natural isotopic background abundance in alanine. (B) Representative chromatogram of cardiac alanine from a mouse 15 min after receiving a 50 mg oral gavage of [U-^{13}C] glucose. Compared with (A), there is an increase in abundance of the M + 3 (221 *m/z*) isotopomer demonstrating ^{13}C glucose derived carbon in this end glycolytic product.

again consistent with our findings in skeletal muscle, such that once insulin resistance develops it does not deteriorate despite continued exposure to a HFD [6]. Moreover, this is consistent with human prospective studies which show that whole body insulin resistance remains constant for many years prior to the development of overt T2D [12,13].

Our assessment of cardiac insulin sensitivity was made using the euglycemic–hyperinsulinemic clamp. While this may be the 'gold standard' technique to measure insulin sensitivity, it does not replicate the dynamic nature of postprandial nutrient metabolism [14]. Therefore we aimed to investigate *in vivo* cardiac glucose metabolism under conditions that better reflect the postprandial state so as to understand how insulin resistance actually impacts intracellular glucose handling beyond the glucose transport process. Based on our clamp studies which established that cardiac insulin resistance develops within 3 weeks of HFD feeding and remains constant for at least up to 16 weeks, we could ensure that selecting a period of fat-feeding for the dynamic metabolic flux profiling studies of between 3 and 16 weeks would cause cardiac insulin resistance.

3.2. Oral [U-^{13}C] glucose challenge

To assess cardiac glucose and intermediary metabolism under dynamic conditions a bolus of [U-^{13}C] glucose was orally administered to mice fed either a chow or HFD for 10 weeks and the heart was excised 15 or 60 min after glucose administration. The use of [U-^{13}C] glucose allowed us to track the movement of glucose derived carbon throughout pathways of intermediary metabolism in the heart via GC–MS based metabolomics. We have recently published findings in skeletal muscle from this study [7] where the theoretical and technical constraints of this experimental protocol have been discussed in detail. Our previous report in these animals demonstrated that, as expected, the HFD mice were heavier than chow controls, and developed glucose intolerance and hyperinsulinemia both basally and during the [U-^{13}C] oral glucose challenge [7]. Furthermore, the plasma ^{13}C glucose tracer kinetics was also reported in this paper [7], revealing that tracer enrichment did not differ between the chow and HFD animals.

3.3. Cardiac metabolic flux profiling

Metabolic flux profiling was determined by examining ^{13}C isotope labelling in glycolytic and TCA cycle metabolites in the heart following [U-^{13}C] glucose administration. The basis of this approach is illustrated in the chromatograms in Fig. 2. Fig. 2A shows alanine labelling 15 min after administration of water (i.e. unlabelled control). Only naturally occurring background isotopic abundance was detected, depicted by the large M + 0 unlabelled isotopomer and corresponding low abundance of the M + 1, M + 2

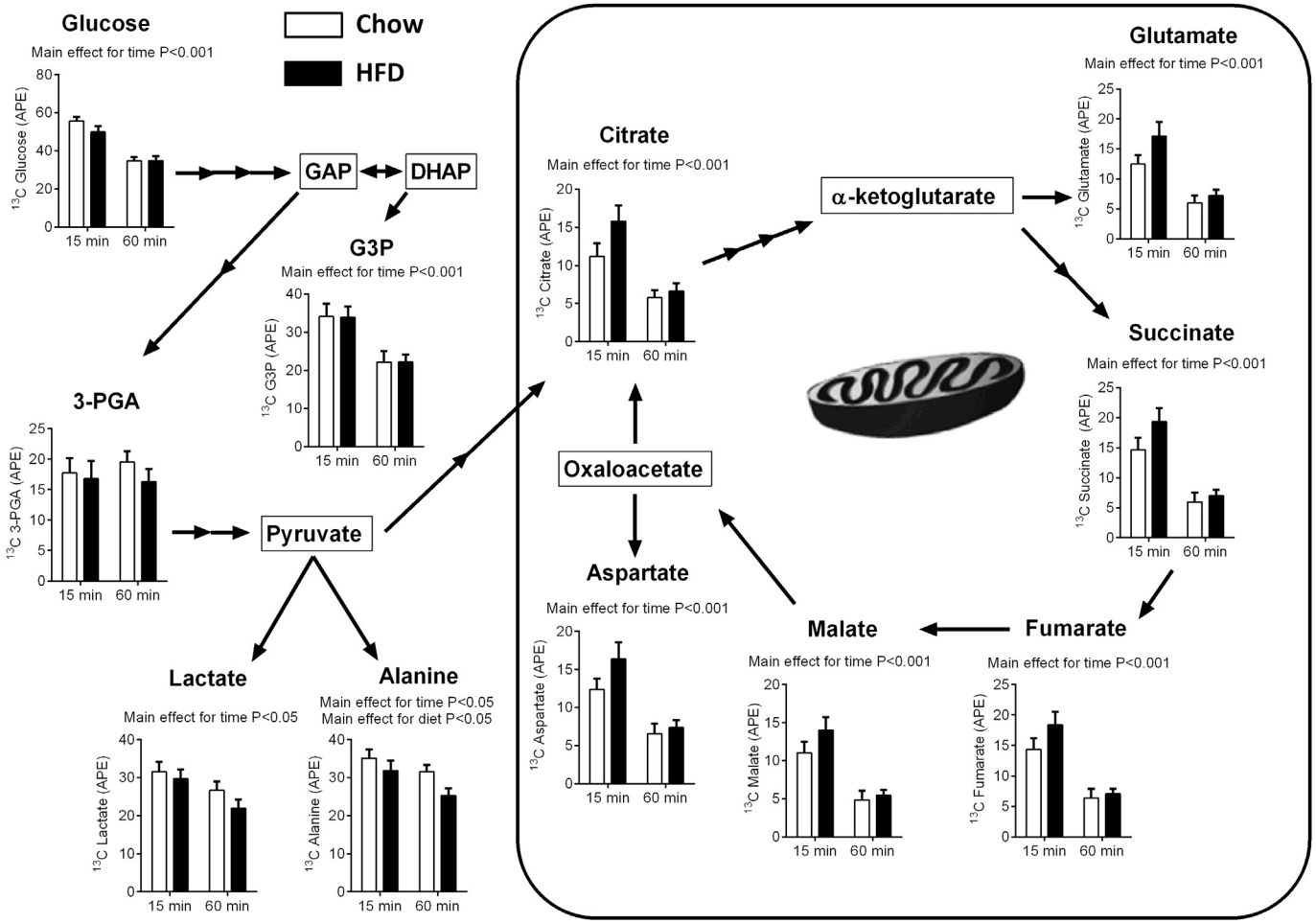

Fig. 3. Dynamic metabolomic profiling of cardiac glucose metabolism. Profiling of cardiac ^{13}C mass isotopomers in glycolytic and TCA cycle intermediates. Data are expressed as atomic percent excess (APE). Data are mean ± SEM. N = 10 chow 15 min, N = 9 chow 60 min, N = 9 HFD 15 min and N = 8 HFD 60 min. Data were analysed by two-way ANOVA. Significance is indicated in each graph. 3PGA; 3-phosphoglycerate, G3P; glycerol 3-phosphate.

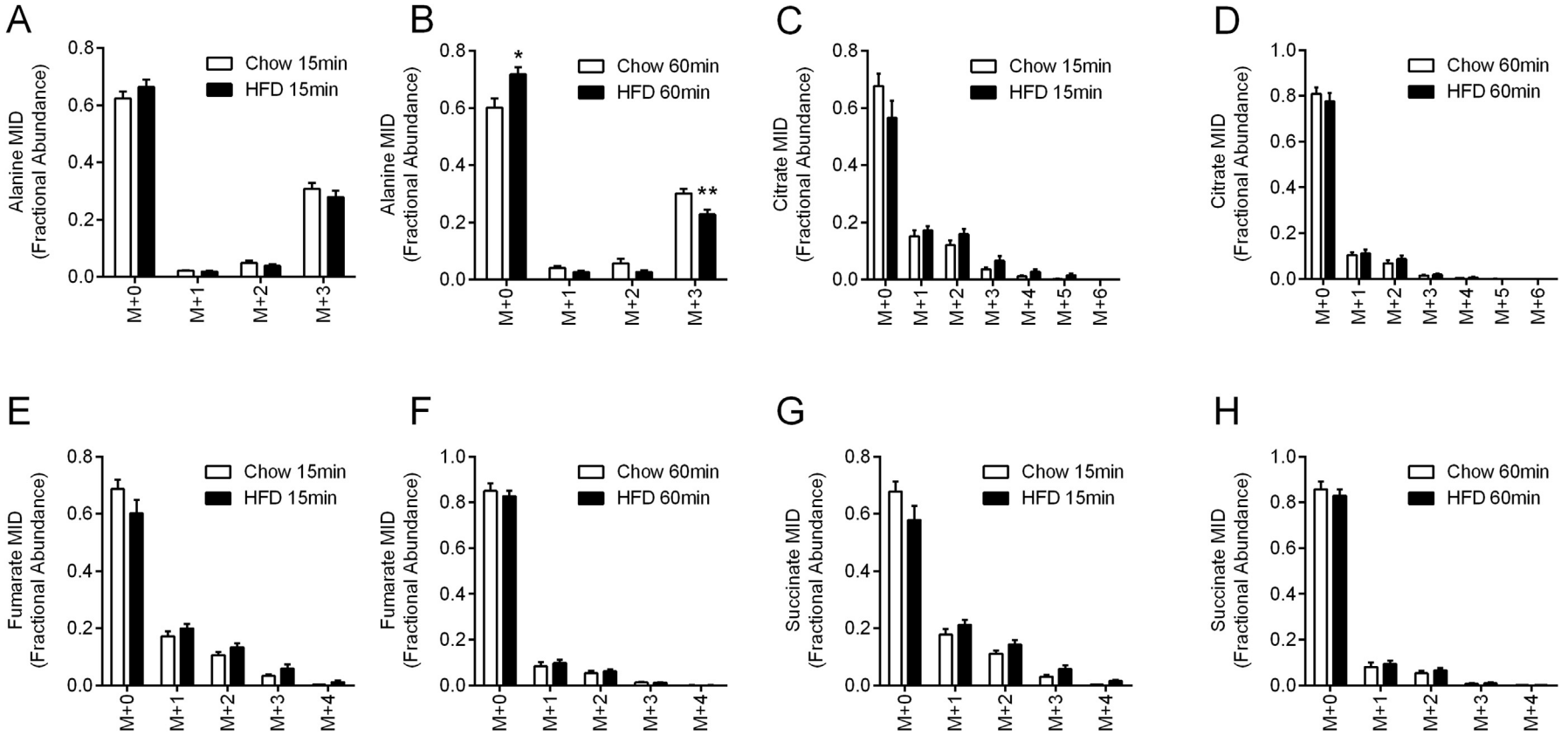

Fig. 4. Cardiac metabolite mass isotopomer distributions (MIDs). (A, B) mass isotopomer distributions (MIDs) of cardiac alanine, (C, D) citrate, (E, F) fumarate and (G, H) succinate. All metabolites in this figure were analysed via their molecular [M-15] TMS derivatized ions. Data are mean ± SEM and presented as fractional abundance in excess of the natural isotopic background. N = 10 chow 15 min, N = 9 chow 60 min, N = 9 HFD 15 min and N = 8 HFD 60 min. Data were analysed by unpaired Student's *t*-test; *P < 0.05.

and virtually absent M + 3 isotopomers. Fig. 2B illustrates alanine labelling 15 min after [U-^{13}C] glucose gavage. Compared with Fig. 2A, there was a marked increase in the abundance of the M + 3 isotopomer, demonstrating orally derived [U-^{13}C] glucose is undergoing glycolysis to form [U-^{13}C] pyruvate, which is in rapid exchange with alanine and is often used as a readout of pyruvate labelling due to its greater chemical stability [15].

Dynamic flux profiling results in the heart are shown in Fig. 3. There was significant labelling in the metabolites of glycolysis and the TCA cycle, with the degree of labelling being strongly influenced by time. Interestingly, in the glycolytic pathway, the HFD only significantly affected ^{13}C labelling in alanine, which was modestly reduced while lactate was unaltered. Although not significant, there was a trend for the HFD mice to have increased labelling in the TCA cycle intermediates 15 min after glucose administration. This shows that despite the presence of cardiac insulin resistance, glucose metabolism in the heart is uncompromised during the oral glucose challenge in HFD fed mice. While this may initially seem counterintuitive, it is likely the cardiac insulin resistance is compensated for by the prevailing hyperglycemia and hyperinsulinemia seen in the HFD fed animals [7]. Such compensation for glucose uptake and oxidation has been shown previously in the heart of humans [16] and mice [17,18] (*db*/*db*) with overt T2D. These findings further emphasize that conclusions drawn from euglycemic–hyperinsulinemic clamp studies need to be reconciled with the fact that the dynamic changes in blood glucose and insulin in the postprandial state play a key role in regulating glucose metabolism, and as such observations from clamp studies do not necessarily reflect metabolic responses following nutrient ingestion. Interestingly, unlike what we observed in the skeletal muscle of these mice, whereby ^{13}C enrichment in both the glycolytic and TCA cycle metabolites remained essentially constant over time [7], the enrichment in the metabolic intermediates of the heart, particularly those of the TCA cycle were markedly (~50%) reduced at the 60 min compared to that of the 15 min time point (Fig. 3). This ~50% reduction in TCA cycle labelling over time occurred despite a high degree of ^{13}C labelling in lactate and alanine, which are in exchange with pyruvate. Thus given pyruvate is the glucose derived carbon source feeding the TCA cycle, and the fact that it remains heavily labelled at 60 min after glucose administration, strongly indicates that fatty acid derived (unlabelled) acetyl-CoA in the heart replaces and hence dilutes the glucose derived ^{13}C labelling in the TCA cycle. This is consistent with the heart being heavily reliant on fatty acid oxidation for energy supply [19], suggesting it only switches to glucose oxidation during the peak levels of hyperglycemia and hyperinsulinemia, thereafter reverting back to the preferential oxidation of fatty acids.

Using the ^{13}C labelling patterns, termed mass isotopomer distributions (MIDs), it was possible to make a qualitative assessment of the pathways by which pyruvate enters the TCA cycle [20], thus providing further insight into cardiac intermediary metabolism. There are two possible points by which pyruvate can enter the TCA cycle; pyruvate decarboxylation and hence formation of acetyl-CoA via pyruvate dehydrogenase (PDH) or carboxylation of pyruvate to oxaloacetate by pyruvate carboxylase, known as TCA cycle anaplerosis [20]. For a more detailed background on assessing pyruvate anaplerosis please see our previous publication [7] and the recent review by Buescher et al. [20]. Briefly, if there is substantial anaplerosis from [U-^{13}C] glucose derived triply labelled pyruvate ([U-^{13}C] pyruvate), the four carbon TCA cycle intermediates (oxaloacetate, aspartate, malate and fumarate) would be expected to exhibit significant M + 3 labelling, and possibly M + 4 labelling due to carryover of acetyl-CoA derived ^{13}C labelling from the PDH reaction. Notably, if there is significant pyruvate anaplerosis, the resulting M + 3 labelled oxaloacetate can be further used in the TCA cycle to generate M + 5 citrate, as M + 3 oxaloacetate could combine with M + 2 acetyl-CoA [20]. In our experiments, we therefore used the MIDs of the molecular (M-15) ions of alanine (readout of pyruvate), citrate, fumarate and succinate to determine pyruvate entry into the TCA cycle as we have done previously in the skeletal muscle of the same animals [7].

Based on the alanine MIDs (Fig. 4A and B) it is clear the bulk of ^{13}C labelling occurs in the m + 3 form, with only the 60 min (Fig. 4B) M + 3 values being modestly altered in the HFD mice. The data indicate that the majority (~80%) of the labelled alanine and hence pyruvate was uniformly (M + 3) labelled for both time points and diets. In the case of cardiac citrate, MIDs indicated the majority of labelling occurred in the M + 1 and M + 2 form (Fig. 4C and D), with M + 3 labelling representing only ~12% and 8% of total labelling at 15 and 60 min respectively, with no significant differences between diets. Analysis of fumarate MIDs (Fig. 4E and F) also revealed that the majority of labelling occurred in the M + 1 and M + 2 forms, with M + 3 representing only ~8% of the total fumarate labelling seen at both time points, with no differences between diets. The same labelling pattern seen in fumarate was also observed in succinate (Fig. 4G and H), indicating negligible pyruvate carboxylation. Therefore the data demonstrate that during an oral glucose challenge, like we previously reported in the skeletal muscle [7], the majority (>95%) of pyruvate enters the cardiac TCA cycle via PDH, with pyruvate TCA cycle anaplerosis being negligible. These results support previous isolated cardiac perfusion studies in rats which demonstrate that very little (<5%) pyruvate enters the TCA cycle via direct carboxylation [21].

In summary, we describe the application of a novel dynamic metabolomics approach to study cardiac glucose metabolism *in vivo*. This provides important insight into the regulation of cardiac glucose metabolism under physiological conditions and unexpectedly revealed that cardiac glucose metabolism, unlike skeletal muscle glucose metabolism [7], is not compromised in HFD mice despite the presence of cardiac insulin resistance, as measured by the euglycemic hyperinsulinemic clamp. The data also reveal that as compared to the skeletal muscle of the same mice [7], cardiac glucose metabolism displays different temporal patterns, particularly at the level of the TCA cycle.

Sources of funding

This work was supported by a grant from the Diabetes Australia Research Trust. RSLY and MJM are supported by fellowships from the National Health and Medical Research Council of Australia (APP1059530).

Disclosures

None.

Acknowledgements

We would like to thank the excellent technical assistance provided by Patricio Sepulveda.

Transparency document

Transparency document related to this article can be found online at http://dx.doi.org/10.1016/j.bbrc.2015.06.019.

References

[1] P. Iozzo, et al., Independent association of type 2 diabetes and coronary artery disease with myocardial insulin resistance, Diabetes 51 (10) (2002) 3020–3024.

[2] I. Yokoyama, et al., Role of insulin resistance in heart and skeletal muscle F-18 fluorodeoxyglucose uptake in patients with non-insulin-dependent diabetes mellitus, J. Nucl. Cardiol. 7 (3) (2000) 242–248.

[3] G. Paternostro, et al., Cardiac and skeletal muscle insulin resistance in patients with coronary heart disease. A study with positron emission tomography, J. Clin. Invest. 98 (9) (1996) 2094–2099.

[4] L.M. Voipio-Pulkki, et al., Heart and skeletal muscle glucose disposal in type 2 diabetic patients as determined by positron emission tomography, J. Nucl. Med. 34 (12) (1993) 2064–2067.

[5] T. Ohtake, et al., Myocardial glucose metabolism in noninsulin-dependent diabetes mellitus patients evaluated by FDG-PET, J. Nucl. Med. 36 (3) (1995) 456–463.

[6] N. Turner, et al., Distinct patterns of tissue-specific lipid accumulation during the induction of insulin resistance in mice by high-fat feeding, Diabetologia 56 (7) (2013) 1638–1648.

[7] G.M. Kowalski, et al., Application of dynamic metabolomics to examine in vivo skeletal muscle glucose metabolism in the chronically high-fat fed mouse, Biochem. Biophys. Res. Commun. 462 (1) (2015) 27–32.

[8] E.W. Kraegen, et al., Dose-response curves for in vivo insulin sensitivity in individual tissues in rats, Am. J. Physiol. 248 (3 Pt 1) (1985) E353–E362.

[9] A. Nanchen, T. Fuhrer, U. Sauer, Determination of metabolic flux ratios from 13C-experiments and gas chromatography-mass spectrometry data: protocol and principles, Methods Mol. Biol. 358 (2007) 177–197.

[10] R.R. Wolfe, D.L. Chinkes, in: second ed., in: N.J. Hoboken (Ed.), Isotope Tracers in Metabolic Research: Principles and Practice of Kinetic Analysis, vol. vii, Wiley-Liss, 2005, p. 474.

[11] S.Y. Park, et al., Unraveling the temporal pattern of diet-induced insulin resistance in individual organs and cardiac dysfunction in C57BL/6 mice, Diabetes 54 (12) (2005) 3530–3540.

[12] D. Jallut, et al., Impaired glucose tolerance and diabetes in obesity: a 6-year follow-up study of glucose metabolism, Metabolism 39 (10) (1990) 1068–1075.

[13] A.G. Tabak, et al., Trajectories of glycaemia, insulin sensitivity, and insulin secretion before diagnosis of type 2 diabetes: an analysis from the Whitehall II study, Lancet 373 (9682) (2009) 2215–2221.

[14] G.M. Kowalski, C.R. Bruce, The regulation of glucose metabolism: implications and considerations for the assessment of glucose homeostasis in rodents, Am. J. Physiol. Endocrinol. Metab. 307 (10) (2014) E859–E871.

[15] U. Sauer, Metabolic networks in motion: 13C-based flux analysis, Mol. Syst. Biol. 2 (2006) 62.

[16] D. Jagasia, et al., Effect of non-insulin-dependent diabetes mellitus on myocardial insulin responsiveness in patients with ischemic heart disease, Circulation 103 (13) (2001) 1734–1739.

[17] A.D. Hafstad, et al., Perfused hearts from type 2 diabetic (db/db) mice show metabolic responsiveness to insulin, Am. J. Physiol. Heart Circ. Physiol. 290 (5) (2006) H1763–H1769.

[18] A.D. Hafstad, et al., Glucose and insulin improve cardiac efficiency and post-ischemic functional recovery in perfused hearts from type 2 diabetic (db/db) mice, Am. J. Physiol. Endocrinol. Metab. 292 (5) (2007) E1288–E1294.

[19] B. Patterson, A.V. Fields, R.P. Shannon, New insights into myocardial glucose metabolism: surviving under stress, Curr. Opin. Clin. Nutr. Metab. Care 12 (4) (2009) 424–430.

[20] J.M. Buescher, et al., A roadmap for interpreting 13C metabolite labeling patterns from cells, Curr. Opin. Biotechnol. 34C (2015) 189–201.

[21] M.E. Merritt, et al., Hyperpolarized 13C allows a direct measure of flux through a single enzyme-catalyzed step by NMR, Proc. Natl. Acad. Sci. U. S. A. 104 (50) (2007) 19773–19777.